ORIGINAL RESEARCH

American Heart Association | American Stroke Association

Apoprotein B, Small-Dense LDL and Impaired HDL Remodeling Is Associated With Larger Plaque Burden and More Noncalcified Plaque as Assessed by Coronary CT Angiography and Intravascular Ultrasound With Radiofrequency Backscatter: Results From the ATLANTA I Study

Szilard Voros, MD, FACC, FSCCT, FAHA;* Parag Joshi, MD; Zhen Qian, PhD; Sarah Rinehart, MD, FACC, FSCCT; Jesus G. Vazquez-Figueroa, MD; Hunt Anderson, MD; Michael Elashoff, PhD; Laura Murrieta, CCRC; Dimitri Karmpaliotis, MD, FACC; Anna Kalynych, MD, FACC; Charles Brown, III, MD, FACC; Ernst Schaefer, MD; Bela Asztalos, PhD

***Background*—**Apoprotein B–containing lipoproteins are atherogenic, but atheroprotective functions of apoprotein A–containing high-density lipoprotein (HDL) particles are poorly understood. The association between lipoproteins and plaque components by coronary computed tomography angiography (CTA) and intravascular ultrasound with radiofrequency backscatter (IVUS/VH) has not been evaluated.

***Methods and Results*—**Quantitative, 3-dimensional plaque measurements were performed in 60 patients with CTA and IVUS/VH. Apoproteins, lipids, and HDL subpopulations were measured with 2-dimensional (2D) gel electrophoresis, and correlation was assessed with univariate and multivariable models. ApoB particles were associated with a higher proportion of noncalcified plaque (NCP) and a lower proportion of calcified plaque (small, dense low-density lipoprotein cholesterol and high-density NCP: r=0.3, P=0.03; triglycerides and low-density NCP: r=0.34, P=0.01). Smaller, dense, lipid-poor HDL particles were associated with a shift from calcified plaque to NCP on CTA (α3-HDL% and low-density NCP: r=0.32, P=0.02) and with larger plaque volume on IVUS/VH (α4-HDL%: r=0.41, P=0.01; α3-HDL%: r=0.37, P=0.03), because of larger dense calcium (α4-HDL%: r=0.37, P=0.03), larger fibrous tissue (α4-HDL%: r=0.34, P=0.04), and larger necrotic core (α4-HDL%: r=0.46, P<0.01; α3-HDL%: r=0.37, P=0.03). Larger lipid-rich HDL particles were associated with less low-density NCP on CTA (α2-HDL%: r=−0.34, P=0.02; α1-HDL%: r=−0.28, P=0.05), with smaller plaque volume on IVUS/VH (pre-α2-HDL: r=−0.33, P=0.05; α1-HDL%: r=−0.41, P=0.01; pre-α2-HDL: r=−0.33, P=0.05) and with less necrotic core (α1-HDL: r=−0.42, P<0.01; pre-α2-HDL: r=−0.38, P=0.02; α2-HDL: r=−0.35, P=0.03; pre-α1-HDL: r=−0.34, P=0.04). Pre-β2-HDL was associated with less calcification and less stenosis by both modalities.

***Conclusions*—**ApoB and small HDL particles are associated with larger plaque burden and more noncalcified plaque, whereas larger HDL and pre-β2-HDL particles are associated with plaque burden and less noncalcified plaque by both CTA and IVUS/VH. **(*J Am Heart Assoc*. 2013;2:e000344 doi: 10.1161/JAHA.113.000344)**

Key Words: atherosclerosis • imaging • lipids • lipoproteins

From the Global Genomics Group, LLC, Richmond, VA (S.V.); Piedmont Heart Institute, Atlanta, GA (P.J., Z.Q., S.R., J.G.V.-F., H.A., L.M., D.K., A.K., C.B.); CardioDx, Inc, Palo Alto, CA (M.E.); Tufts University Medical Center, Boston, MA (E.S., B.A.).

*Dr. Voros is now located at Stony Brook University; Stony Brook, NY.

Correspondence to: Szilard Voros, MD, FACC, FSCCT, FAHA, Global Genomics Group, LLC, 737 North 5th Street, Suite 103, Richmond, VA 23219. E-mail: szilardvorosmd@gmail.com

Received June 1, 2013; accepted October 7, 2013.

Atherosclerosis is responsible for coronary artery disease (CAD), which remains the leading cause of morbidity and mortality worldwide.[1] One of the first steps in the atherosclerotic process is the deposition and retention of atherogenic lipoprotein particles in a susceptible coronary arterial vessel wall, followed by a reactive inflammatory process, smooth muscle cell proliferation, fibrosis, and calcification.[2] On the other hand, lipoproteins associated with reverse cholesterol transport are able to remove excess cholesterol from macrophages in atherosclerotic plaques, providing an atheroprotective mechanism.

Lipoprotein particles are composed of lipid components such as cholesterol, cholesteryl-esters, phospholipids, and

triglycerides and protein components such as apoprotein B (apoB), apoprotein A (apoA), apoprotein C, and apoprotein E. The central principle of the atherogenic dyslipidemia paradigm is that apoB-containing particles are atherogenic because of the physical binding of apoB to proteoglycans in the vessel wall. In contrast, apoAI-containing high-density lipoprotein (HDL) particles are atheroprotective by removing cholesterol from macrophages in the vessel wall and by preventing low-density lipoprotein (LDL) oxidation and the maladaptive inflammatory response. ApoAI is primarily synthesized in the liver and intestines and is secreted into circulation, where it undergoes a series of remodeling steps facilitated by a number of enzymes such as plasma lipid transfer protein, lecithin-cholesterol acyltransferase, and cholesterol ester transfer protein). Native apoAI gradually acquires phospholipid and becomes pre-β1-HDL, whereas further acquisition of cholesterol and apoAI facilitates remodeling to initially smaller, alpha-migrating α4-HDL. α4-HDL matures to more lipid-rich and larger α3-, α2-, and α1-HDL particles (Figure 1). The large, cholesterol-rich α2- and α1-HDL particles can unload excess cholesterol in the liver through the scavenger receptor–B1 pathway (Figure 1).

HDL subpopulations can be quantitatively measured and characterized by native 2D gel electrophoresis, immunodetection, and image analysis. Certain subpopulations have been shown to be associated with either lower or higher risk of coronary heart disease based on angiographic[3] and outcomes studies.[4,5]

Coronary atherosclerotic plaque can be characterized invasively by intravascular ultrasound (IVUS) with radiofrequency backscatter analysis (IVUS/VH).[6] More recently, contrast-enhanced coronary computed tomography angiography (CTA) has been introduced as a noninvasive means for this purpose.[7–10] Over past years, our laboratory has developed and validated a standardized, 3-dimensional quantitative method for CTA-based coronary plaque quantification and published its reproducibility[8] as well as its accuracy.[11]

However, the relationship between quantitative, 3-dimensional coronary plaque measurements by IVUS/VH and CTA and precise lipoprotein and HDL subpopulation measurements has not previously been evaluated. Therefore, the objective of our study was to study the association between circulating apoB- and apoAI-containing lipoprotein particles and quantitative coronary plaque composition as measured by IVUS/VH and CTA. We hypothesized that apoB-containing lipoprotein particles are associated with a higher-risk phenotype, whereas adequate maturation or dynamic remodeling of apoAI-containing HDL particles ia associated with a lower-risk plaque phenotype, as measured by IVUS/VH and CTA.

Methods

General Study Design

This was a prospective, investigator-initiated, single-center study approved by the Institutional Review Board of Piedmont Healthcare; all patients provided written informed consent. The overall study design has been published previously.[11] Briefly,

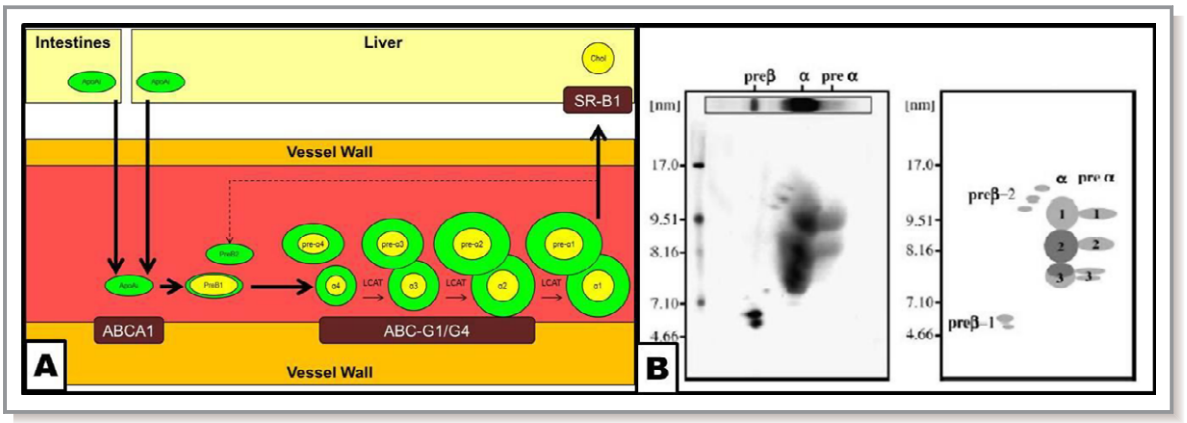

Figure 1. Schematic representation of reverse cholesterol transport and remodeling of apoA-containing HDL particles and 2D gel electrophoresis of HDL particles. A, apoA is synthesized in the intestines and the liver and secreted into circulation. ApoAI interacts with the arterial vessel wall through the ABCA1 transporter, acquires cholesterol, and is remodeled into a discoid, small, relatively lipid-poor pre-β1-HDL particle. Further acquisition of lipids transforms pre-β1-HDL into a small, dense, lipid-poor, spherical α4-HDL particle, accompanied by a pre-α4-HDL particle. The α4-HDL particle interacts with the arterial wall through the ABCG1/G4 transporter system, acquires further lipids, and under the influence of LCAT, lipoprotein lipase (LPL), hepatic lipase (HL), CETP, and PLTP remodels into progressively larger HDL particles, such as α3- and α2-HDL, accompanied by their respective pre-α-migrating particles. Finally, the large, lipid-rich, spherical α1-HDL particle interacts with the SRB-1 receptor in the liver, thus unloading cholesterol to the hepatocytes. The remaining lipid-poor apoA-containing particle may reenter the cycle as a pre-β-migrating particle. B, 2D gel electrophoresis of apoA-containing HDL particles (B, left) and a schematic representation of the different subclasses (B, right). ABCA indicates ATP-binding cassette transporter subfamily A; ABCG1/G4, ATP-binding cassette transporter subfamily G member 1/member 4; CETP, cholesterol ester transfer protein; Chol, cholesterol; HDL, high-density-lipoprotein; LCAT, lecithin-cholesterol acyltransferase; PLTP, plasma lipid transfer protein; SR-B1, scavenger receptor B1.

enrollment criteria were (1) being male or female 18 to 70 years old; (2) having no prior known obstructive CAD; (3) having symptoms suggestive of myocardial ischemia or a high probability of CAD; and (4) having ≥1 "intermediate" coronary artery stenosis present, defined by either CTA (40% to 70% luminal stenosis by CTA criteria) or invasive x-ray angiography (40% to 70% luminal stenosis by angiographic criteria), and lacking obstructive stenosis (>70% luminal stenosis) in the 4 major epicardial arteries. For the entire study, all patients underwent biomarker testing and CTA and IVUS/VH at baseline and then biomarker testing and CTA 12 months later. Blood samples were drawn either at the time of the invasive angiogram or immediately prior to CTA. For the purposes of the current analysis, we analyzed associations between biomarkers, CTA, and IVUS/VH at the baseline examination.

CTA Image Acquisition

All image acquisition was performed on a 32×2 CT system (Siemens Somatom 64; Erlangen, Germany) using our institutional imaging protocols as published before.[11] Contrast-enhanced coronary artery CTA was performed during end-expiratory breath hold using retrospective ECG gating. Oral and intravenous metoprolol were administered as needed to keep the heart rate <60 beats per minute. After noncontrast localization image acquisition, a test bolus of 20 mL iodinated contrast (Visipaque, GE Amersham Health) was administered at a rate of 3 to 5 mL/s to determine the delay until the arrival of the contrast in the ascending aorta for optimal opacification of the coronary arteries. Coronary arterial image acquisition was performed using 60 to 80 mL of intravenous contrast followed by 30 mL of normal saline flush. Acquisition parameters included 32×2 detector rows, 0.6-mm collimation, gantry rotation of 330 ms, pitch of 0.24, tube voltage of 120 kV, and tube current of 800 to 950 mA. Images were reconstructed in 0.6-mm axial slices using 3 different reconstruction algorithms in 10 phases of the cardiac cycle.

CTA Image Analysis

Selected for image analysis in each patient was a target vessel segment that contained the preidentified intermediate coronary artery lesion (40% to 70% luminal stenosis) in the preenrollment CTA or x-ray angiography examination, as previously described.[8,11] Starting and termination points of the target segment were precisely defined on the basis of a modified 13-segment coronary arterial model using distinguishable vessel ostia and branch points, including the diagonal branches in the left anterior descending artery, the marginal branches in the left circumflex artery, and the right ventricular marginal branches in the right coronary artery. When such branches were not present, the epicardial artery was divided into respective equidistant segments.

Lumen and vessel geometry and composition were quantitatively evaluated in a 3-dimensional fashion in the target vessel segment using our previously described standardized approach (SurePlaque; Vitrea 4.0; Vital Images).[8,11] Geometrical parameters measured and calculated included segment length, minimal luminal diameter, minimal luminal area, percent luminal diameter stenosis, and percent luminal area stenosis. Percent luminal diameter stenosis was calculated as $(\text{diameter}_{\text{lesion}}/\text{diameter}_{\text{mean reference}})\times 100$, where mean reference was the minimal lumen diameter in the cross-sectional slices with the preidentified lesion, and was calculated by averaging the luminal diameters of proximal and distal reference slices to correct for vessel tapering. Proximal and distal reference slices were defined as normal slices or the slices with the least amount of discernible plaque in the proximal and distal portions of the segment. Similarly, we defined percent luminal area stenosis as $(\text{area}_{\text{lesion}}/\text{area}_{\text{mean reference}})\times 100$, where lesion slice and reference slices were the same as for the percent luminal diameter stenosis calculations.

Within the vessel wall area of the target vessel segment, plaque composition was quantified based on predefined Hounsfield unit (HU) thresholds. Plaque was classified as calcified with a density >150 HU. Noncalcified plaque (NCP) was divided into 2 categories: NCP with attenuation values <30 HU were classified as low-density NCP and NCP with attenuation values in the range of 31 to 150 HU was classified as high-density NCP. The total volume and the percentage of each plaque component were determined.

IVUS/VH Image Acquisition

After intracoronary injection of nitroglycerin (mean total dose per case, 561.5 μg; range, 0 to 1800 μg) and after placing a guiding catheter in the target coronary artery, a 3.2F, 20-mHz ultrasound catheter (Eagle Eye; Volcano Inc, Rancho Cordova, CA) was inserted and was advanced at least 2 cm beyond the most distal portion of the target lesion. Automated pullback was performed at a rate of 0.5 mm/s (R-100; Volcano Inc, Rancho Cordova, CA). The electrocardiographic signal was simultaneously recorded for the reconstruction of the radiofrequency backscatter information using In-Vision Gold (Volcano Inc, Rancho Cordova, CA).

IVUS/VH Image Analysis

Deidentified IVUS/VH data sets were transferred to a dedicated workstation and were analyzed using dedicated software (pcVH 3.0.394; Volcano Inc, Rancho Cordova, CA) by an experienced cardiologist (G.V.). The luminal boundary and the external elastic lamina were contoured in a semiautomatic

fashion in each frame. On the basis of a previously validated algorithm, the software classified each pixel as dense calcium (white), fibrous tissue (green), fibrofatty tissue (light green), and necrotic core (red). Total volume and percentages of each of the 4 components were measured in the study segment. Furthermore, we calculated the volume and percentages of all noncalcified plaque components (sum of necrotic core, fibrofatty tisue, and fibrous tissue).

Lipoprotein Measurements

Blood was collected from all participants at either the time of the index CTA examination or the invasive angiographic procedure, whichever occurred first. Plasma samples were separated by low-speed centrifugation, aliquoted, and frozen at −80°C within an hour. All samples were analyzed as a single batch in a core laboratory (Boston Heart Laboratory, Framingham, MA) to maintain consistency. Total cholesterol, LDL-C, HDL-C, and triglycerides were measured with standard enzymatic methods and apoB, apoAI, and Lp(a) by immunoturbimetric methods. HDL subpopulations, including pre-β1-, pre-β2-, α1-, α2-, α3-, α4-, pre-α1-, pre-α2-, pre-α3, and pre-α4-HDL, were measured by nondenaturing, 2D gel electrophoresis and image analysis as validated and published previously.[3] Briefly, in the first dimension, HDL particles were separated based on charge into pre-β, α, and pre-α mobility fractions, using albumin as reference. In the second dimension, HDL particles were separated by size (pre-β1 to -2, α1 to α 4, and pre-α1 to α4). Gels were electrotransferred to nitrocellulose membranes followed by immunolocalization with monospecific primary and ^{125}I-labeled secondary antibodies. Quantitative image analysis of the 2D gel allows the quantification of the percent distribution of apoAI-containing HDL subpopulations. ApoAI concentrations (mg/dL) in the individual HDL subpopulations were calculated by multiplying the percentile by the plasma total ApoAI level.

Statistical Analysis

Continuous variables are expressed as mean±standard deviation and median (interquartile range). Pearson correlation coefficient (*r*) was determined using standard methods. Univariate associations between lipoprotein measurements and plaque parameters were estimated using linear regression models. Unless otherwise noted, relationships between lipoprotein measurements and plaque parameters were approximately linear. Adjusted associations were estimated using multivariable linear regression models that included age, sex, BMI, diabetes, and medication usage. For all analyses, $P \leq 0.05$ was considered statistically significant, with no adjustment for multiple comparisons.

Results

General Demographic Parameters

Overall, 60 patients were enrolled in the study (Table 1). In the entire cohort, mean age was 60.4±7.2 years; 60% were male. Although greater than 70% of patients enrolled had cardiovas-

Table 1. General Demographic Parameters

Characteristic	Frequency, Value, or IQR
Subjects	n=60
Age, mean±SD	60.4±7.2
Men (%)	36 (60%)
Ethnicity	
White	55 (91.7%)
African American	5 (8.3%)
Risk factors	
Hypertension	50 (83.3%)
Dyslipidemia	58 (96.7%)
Tobacco use (former or current)	35 (58.3%))
Diabetes mellitus	44 (73.3%)
Framingham Risk Score (10-year risk; mean±SD)	8.2±6.1
Symptoms	
Chest pain (angina)	27 (45%)
Shortness of breath	16 (26.7%)
Medications	
Aspirin	43 (71.7%)
Beta-blocker	30 (50%)
Angiotensin-converting enzyme inhibitor	18 (30%)
Angiotensin receptor blocker	6 (10%)
Nitrate	6 (10%)
Statin	40 (66.7%)
Cholesterol absorption inhibitor	15 (25%)
Niacin	9 (15%)
Fibric acid derivative	3 (5%)
Laboratory values	
Total cholesterol, mg/dL	154.6±47.9 (124 to 172)
ApoB, mg/dL	78.4±29.8 (59.7 to 91.5)
LDL cholesterol, mg/dL	87.5±37.4 (59.2 to 107.1)
sd-LDL-C, mg/dL	14.8±10.8 (6.8 to 18.6)
ApoAI, mg/dL	141.3±31.6 (126.3 to 154.3)
HDL cholesterol, mg/dL	37.7±10.9 (30.7 to 41.9)
Triglycerides, mg/dL	127.3±60.9 (79.7 to 164)

HDL indicates high-density lipoprotein; IQR, interquartile range; LDL, low-density lipoprotein; SD, standard deviation; sd-LDL, small, dense low-density lipoprotein.

Table 2. ApoA-Containing HDL Subclass Distribution in Patients at Baseline

HDL Particle	Absolute Value, SD, and IQR (mg/dL)	Percentage, SD, and IQR
pre-β1-HDL	18.8±7.9 (12.4 to 23.4)	13.0±4.2 (10 to 15.7)
pre-β2-HDL	2.0±1.4 (0.9 to 2.6)	1.4±1.0 (0.6 to 1.9)
pre-α1-HDL	2.9±3.0 (1.0 to 3.7)	1.9±1.9 (0.7 to 2.4)
α1-HDL	13.2±9.2 (6.7 to 18.1)	8.9±5.3 (5.1 to 11.9)
pre-α2-HDL	5.1±3.1 (3.1 to 6.6)	3.5±1.8 (2.5 to 4.6)
α2-HDL	49.5±14.5 (38.6 to 62)	34.5±5.7 (30.2 to 37.2)
pre-α3-HDL	2.9±1.8 (1.8 to 3.2)	2.1±1.4 (1.3 to 2.4)
α3-HDL	33.7±9.3 (26.8 to 41.5)	24.5±7.9 (18.4 to 28.2)
pre-α4-HDL	1.1±0.7 (0.6 to 1.5)	0.8±0.5 (0.4 to 0.9)
α4-HDL	12.9±4.2 (9.7 to 15.5)	9.3±3.0 (7 to 11)

HDL indicates high-density lipoprotein; IQR, interquartile range; SD, standard deviation.

cular risk factors of diabetes, dyslipidemia and/or diabetes, the mean FRS was low (8.2±6.1), presumably because of treatment. Most patients were on lipid-lowering medications at the time of enrollment, as shown in Table 1. Lipoprotein parameters, including each of the lipoprotein subclasses, at the time of imaging are shown in Table 2.

Biomarkers and Plaque Characteristics by CTA

Plaque geometrical and compositional parameters in the overall CTA cohort are shown in Table 3 and Figure 2A and 2B. Results of unbiased heat-map analysis are shown in Figure 3A. In general, apoB-related measurements and apoB-containing particles were associated with a shift in plaque composition from a lower proportion of calcified to a higher proportion of noncalcified plaque components (Table 4). In univariate analysis, apoB was associated with less calcified plaque (r=−0.33, P=0.02), more high-density NCP (r=0.31, P=0.03), and more low-density NCP (r=0.29, P=0.04); see Figure 4. sd-LDL-C was associated with a smaller percentage of calcified plaque (r=−0.30, P=0.03) and a higher percentage of high-density NCP (r=0.30, P=0.03), whereas triglycerides were associated with a higher percentage of low-density NCP (r=0.34, P=0.01).

Smaller, lipid-poor HDL particles (pre-α4-HDL, pre-α3-HDL, and α3-HDL) were associated with a lower proportion of calcified and a higher proportion of noncalcified plaque components (for high-density NCP%: pre-α3-HDL, r=0.40, P<0.01; pre-α4-HDL, r=0.29, P=0.04; for low-density NCP%: α3-HDL%, r=0.32, P=0.02; Table 4; Figure 5).

Larger, lipid-rich HDL particles (α2-HDL and α1-HDL) were associated with a lower proportion of low-density NCP% (α2-HDL%, r=−0.34, P=0.02; α1-HDL%, r=−0.28, P=0.05). Also, overall HDL-C measurements were associated with a lower proportion of low-density NCP on univariate analysis (r=−0.34, P=0.01; Table 4; Figure 5).

Finally, pre-β2-HDL particles were associated with lower volume of calcified plaque (r=−0.29, P=0.04) and less stenosis (minimal luminal diameter, r=0.30, P=0.03; percent diameter stenosis, r=−0.30, P=0.03) see Table 5 and Figure 6. Importantly, several of the lipoproteins remained significant in the multivariable analysis after adjusting for age, sex, BMI, diabetes, and medications (Table 4).

Table 3. CTA Characteristics of Coronary Atherosclerotic Plaques

CTA Parameter	Value, SD, IQR
MLD, mm	1.6±0.6 (1.2 to 1.9)
% Diameter stenosis	47.1±16.7 (34.5 to 61.5)
MLA, mm^2	5.5±2.5 (3.7 to 6.7)
Area stenosis, %	49.9±18.0 (38.5 to 60.5)
Lesion length, mm	27.9±14.2 (18.9 to 35.3)
Lesion plaque volume, mm^3	234.0±132.1 (138.5 to 294.5)
Calcified plaque volume, mm^3	75.1±70.2 (19.7 to 130.8)
High-density NCP volume, mm^3	139.7±73.7 (93.4 to 170.2)
Low-density NCP volume, mm^3	19.2±12.7 (11.4 to 22)
Calcified plaque, %	28.9±17.8 (12.6 to 43.5)
High-density NCP, %	62.6±16.1 (50.5 to 77.1)

CTA indicates computed tomography angiography; IQR, interquartile range; MLA, minimal lumen area; MLD, minimal luminal diameter; NCP, noncalcified plaque; SD, standard deviation.

Biomarkers and Plaque Characteristics by IVUS/VH

Plaque geometrical and compositional parameters in the overall IVUS/VH cohort are shown in Table 5. Results of unbiased heat-map analysis are shown in Figure 3B. Of the apoB-containing particles, Lp(a) was associated with larger plaque volume by IVUS/VH both in univariate analysis (r=0.42, P=0.01) and in multivariable analysis (β=2.7, P<0.03), mostly because of higher volume of fibrous tissue (r=0.38, P=0.02; β=1.0, P=0.08). In addition, LDL-C was also associated with a higher volume of fibrous tissue (r=0.34, P=0.04; Table 6).

Smaller, lipid-poor HDL particles (α4-HDL and α3-HDL) were associated with higher plaque volume (α4-HDL%, univariate r=0.41, P=0.01; multivariable β=26.4, P=0.02; α3-HDL%, r=0.37, P=0.03). Percentage of α4-HDL was associated with higher volume of dense calcium (r=0.37, P=0.03), higher volume of fibrous tissue (r=0.34, P=0.04), and higher volume of necrotic core (univariate r=0.46, P<0.01; multivariable β=5.1, P=0.02). Percentage of α3-HDL was

Table 4. Correlation Analysis Between Lipoproteins and CTA-Derived Quantitative Coronary Atherosclerotic Plaque Parameters.

	Biomarker	Univariate *r* Value	Univariate *P* Value	Multivariable β-Coefficient	Multivariable *P* Value	Adjusted *P* Value
CAP Volume	Pre-α3-HDL	−0.28	0.05	−8.36	0.12	0.12
	Pre-β2-HDL%	−0.29	0.04	−24.65	0.02	0.02
	Pre-β2-HDL	−0.29	0.04	−16.66	0.02	0.02
CAP%	Pre-α4-HDL	−0.28	0.04	−4.14	0.24	0.24
	Pre-α4-HDL%	−0.28	0.05	−7.14	0.13	0.13
	TC	−0.29	0.04	−0.02	0.77	0.77
	sd-LDL	−0.30	0.03	−0.31	0.19	0.19
	ApoB	−0.33	0.02	−0.08	0.47	0.47
	Pre-α3-HDL	−0.37	<0.01	−2.93	0.03	0.03
	Pre-α3-HDL%	−0.37	<0.01	−4.4	0.01	0.01
HD-NCP%	Pre-α3-HDL	0.40	<0.01	2.98	0.01	0.01
	Pre-α3-HDL%	0.39	<0.01	4.32	<0.01	<0.01
	ApoB	0.31	0.03	0.07	0.46	0.46
	sd-LDL	0.3	0.03	0.3	0.17	0.17
	Pre-α4-HDL	0.29	0.04	3.99	0.21	0.21
	TC	0.27	0.05	0.02	0.76	0.76
LD-NCP%	Triglycerides	0.34	0.01	0.01	0.18	0.18
	A3-HDL%	0.32	0.02	0.12	0.10	0.10
	ApoB	0.29	0.04	0.01	0.7	0.7
	TC	0.24	0.08	0	0.91	0.91
	HDL-C	−0.34	0.01	−0.1	0.07	0.07
	A2-HDL%	−0.34	0.02	−0.16	0.12	0.12
	A1-HDL%	−0.28	0.05	−0.12	0.20	0.20
MLA	Lp(a)	0.27	0.05	0.02	0.08	0.08
%AS	Lp(a)	−0.14	0.31	−0.05	0.64	0.64
	Pre-α2-HDL	−0.30	0.03	−1.17	0.23	0.23
MLD	Lp(a)	0.23	0.10	0	0.32	0.32
	Pre-α2-HDL	0.04	0.77	−0.03	0.28	0.28
	Pre-β2-HDL%	0.30	0.03	0.21	0.02	0.02
%DS	Pre-α2-HDL%	−0.28	0.05	−1.33	0.32	0.32
	Pre-α3-HDL	−0.29	0.04	−1.88	0.11	0.11
	Pre-β2-HDL	−0.30	0.03	−3.27	0.04	0.04

Adjusted *P* values represent adjusting for age, sex, BMI, diabetes, and medication use. One multivariable model was fit for each biomarker separately. AS indicates area stenosis; BMI, body mass index; CAP, calcified plaque; CTA, computed tomography angiography; DS, diameter stenosis; HDL, high-density lipoprotein; HD-NCP, high-density noncalcified plaque; LD-NCP, low-density noncalcified plaque; Lp(a), lipoprotein a; MLA, minimal luminal area; MLD, minimal lumen diameter; sd-LDL, small, dense low-density lipoprotein; TC, total cholesterol.

associated with higher volume of necrotic core (r=0.37, P=0.03; Table 6; Figure 5).

On the other hand, larger, lipid-rich HDL particles (pre-α2-HDL, α2-HDL, pre-α1-HDL, and α1-HDL particles) were associated with lower plaque volume (Table 6; Figure 5), mostly because of a lower volume of dense calcium (pre-α2-HDL, r=−0.33, P=0.05), lower volume of fibrous tissue (pre-α1-HDL, univariate r=−0.39, P=0.02; multivariable β=−11.9, $P\leq$0.01; α1-HDL, r=−0.37, P=0.03), fibrofatty tissue (pre-α1-HDL, r=−0.34, P=0.05), and, importantly, lower volume of necrotic core (α1-HDL, r=−0.42, P<0.01; pre-α2-HDL, r=−0.38, P=0.02; α2-HDL, r=−0.35, P=0.04; and pre-α1-HDL, r=−0.34, P=0.04).

Of the β-migrating HDL particles, pre-β2-HDL particles were associated with a shift in plaque composition to a lower proportion of necrotic core (univariate r=−0.44, P<0.01;

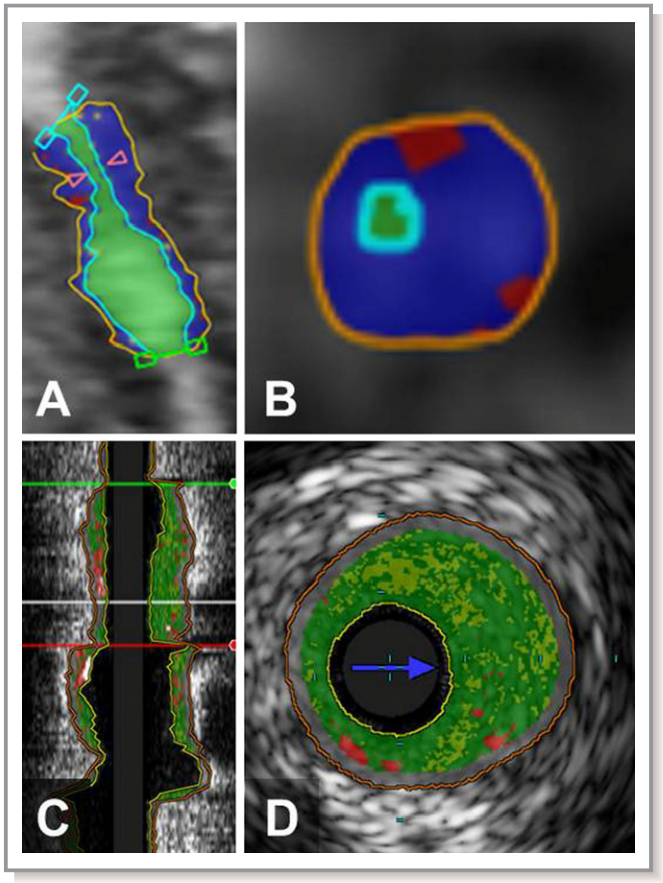

Figure 2. Example of CTA and IVUS/VH analysis of coronary arterial lesions. Long-axis (A) and short-axis (B) views of coronary plaques by CTA, demonstrating the lumen (light green), high-density noncalcified plaque (blue), and low-density noncalcified plaque (red). Corresponding long-axis (C) and short-axis (D) views of the same lesion by IVUS/VH, demonstrating fibrous tissue (dark green), fibrofatty tissue (light green), necrotic core (red), and calcium (white). CTA indicates computed tomography angiography; IVUS/VH, intravascular ultrasound virtual histology.

multivariable β=−1.6, P=0.03) and dense calcium (univariate r=−0.44, P<0.01; multivariable β=−1.6, P<0.03) to a higher proportion of fibrous tissue (univariate r=0.53, P<0.01; multivariable β=3.47, P<0.01). Finally, pre-β2-HDL particles were associated with a lower percentage of area stenosis (r=−0.32, P=0.03) and a lower percentage of diameter stenosis (r=−0.30, P=0.05); see Table 6 and Figure 6. Importantly, several of the lipoproteins remained significant in the multivariable analysis after adjusting for age, sex, BMI, diabetes, and medications (Table 4).

Discussion

In the current study, we used a unique, standardized, quantitative CTA postprocessing method that we have validated in the past both for reproducibility,[8,10] and for accuracy.[11] Similarly, we used an IVUS/VH method that has also been validated in the past by our laboratory[11] and by other laboratories.[12] We also measured lipids and lipoproteins, including sd-LDL-C and the apoAI-containing HDL subpopulations with a previously validated methodology.[3–5]

The present study has 2 significant aspects. First, circulating levels of lipoprotein particles were mostly associated with noncalcified plaque, particularly low-density-NCP on CTA, which is the presumed lipid-rich component.[11,13–15] This is important because it provides external validation that noncalcified regions of atherosclerotic plaques may be directly related to deposition of circulating lipoproteins. Second, the results of CTA-based and IVUS/VH-based plaque characteristics were essentially identical, providing further external validation of the findings.

Our study has 4 important findings. First, apoB-containing lipoprotein particles were associated with a higher proportion of noncalcified and a lower proportion of calcified plaque components. On CTA, sd-LDL-C was associated with a higher proportion of high-density NCP and triglycerides with a higher proportion of low-density NCP, and on IVUS, Lp(a) was associated with a higher plaque volume, mostly because of more fibrous tissue. Second, small, dense, lipid-poor apoA-containing HDL particles were associated with a higher proportion of noncalcified and a lower proportion of calcified components. On CTA, pre-α4-HDL and pre-α3-HDL were associated with a higher proportion of noncalcified components, mostly with high-density NCP. On IVUS, such particles were associated with a larger plaque volume because of a higher volume of dense calcium (α4-HDL), a higher volume of fibrous tissue (α4-HDL), and importantly, a higher volume of necrotic core (α4-HDL, α3-HDL). Third, large, lipid-rich apoA-containing HDL particles were associated with less low-density NCP on CTA and with lower plaque volume on IVUS because of a lower volume of dense calcium (pre-α2-HDL), a lower volume of fibrous tissue (pre-α1-HDL, α1-HDL), a lower volume of fibrofatty tissue (pre-β1-HDL), and importantly, a lower volume of necrotic core (pre-α2-HDL, α2-HDL, pre-α1-HDL, α1-HDL). Finally, pre-β2-HDL particles were associated with less calcification and less stenosis; on IVUS, pre-β2-HDL was associated with a lower proportion of dense calcium and necrotic core and a higher proportion of fibrous tissue.

Our working model of HDL maturation/remodeling is summarized in Figure 1. The major apolipoprotein component of HDL, apoAI, is synthesized in the liver and in the small intestine and is secreted to the circulation in a lipid-free form. ApoAI gains some phospholipids in the circulation and turns into pre-β1-HDL. Pre-β1-HDL is capable of promoting cholesterol efflux from resident macrophages in atherosclerotic plaques via the ABCA1 pathway, resulting in the formation of α4-HDL particles, which are still poorly lipidated, discoidal particles.[16] Through multiple steps, several enzymes including lecithin-cholesterol acyltransferase, lipoprotein lipase (LPL),

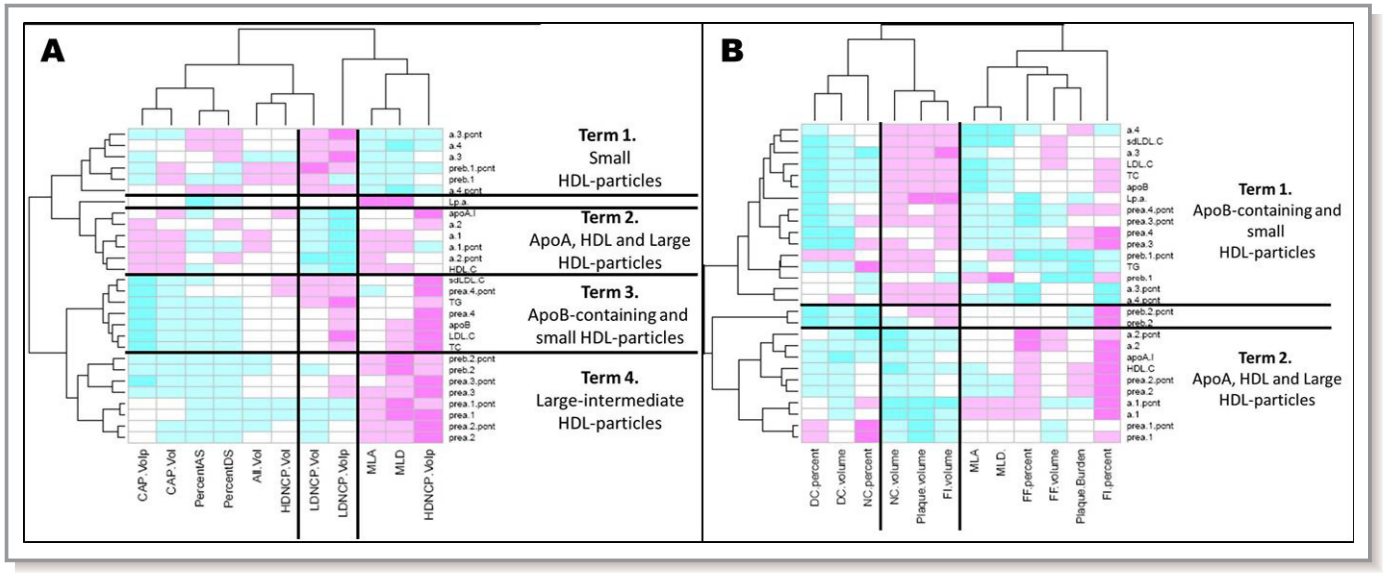

Figure 3. Heat plots illustrating the unbiased grouping of biomarkers in relation to plaque composition by CTA (A) and IVUS/VH (B). On CTA (A), there are 4 major terms. Term 1 contains small HDL particles and is associated with more low-density NCP and more stenosis. Term 2 contains apoA, HDL-C, and large HDL particles and is associated with less low-density NCP and more calcification and less stenosis. Term 3 contains apoB-containing particles and small HDL particles and is associated with more low-density NCP and less calcification. Term 4 contains large HDL particles and is associated with less low-density NCP, less calcified plaque, and less stenosis. On IVUS/VH (B), there are 2 major terms. Term 1 contains apoB-containing particles and small HDL particles and is associated with more necrotic core, larger plaque, and more stenosis. Term 2 contains apoA, HDL-C, and large HDL particles and is associated with less necrotic core and less calcium, more fibrous tissue, and smaller plaque. AS indicates area stenosis; CAP, calcified plaque; CTA, computed tomography angiography; DC, dense calcified; DS, diameter stenosis; FF, fibrofatty; FI, fibrous tissue; HDL, high-density-lipoprotein; HD-NCP, high-density noncalcified plaque; IVUS/VH, intravascular ultrasound virtual histology; LDL, low-density lipoprotein; LD-NCP, low-density noncalcified plaque; Lp(a), lipoprotein a; MLA, minimal lumen area; MLD, minimal lumen diameter; NC, necrotic core; NCP, noncalcified plaque; TC, total cholesterol; TG, triglycerides; sd-LDL, small dense low-density lipoprotein.

hepatic lipase (HL), cholesterol ester transfer protein, and plasma lipid transfer protein transform α-4 HDL particles into larger, more lipidated, spherical HDL particles (α3-, α2-, and α1-HDL with increasing size, respectively). Intermediate-size α3-HDL particles are able to promote more cell-cholesterol efflux via the ABCG1 pathway. The 2 largest HDL subpopulations, α1- and α2-HDL, are able to promote bidirectional cell-cholesterol flux via the scavenger receptor–B1 pathway. Whether these large HDL particles are cholesterol donors or acceptors depends on the lipid status of the macrophages. Cholesterol-loaded cells donate cholesterol to these HDL particles, whereas cholesterol-depleted cells acquire cholesterol from them. Cholesterol uptake by pre-β1-HDL particles via the ABCA1 pathway is the first step and selective cholesterol download by α1-HDL and α2-HDL particles via the liver scavenger receptor–B1 pathway the last step in direct reverse cholesterol transport.

In this context, our study found that higher levels of smaller, immature HDL particles (pre-α4-HDL, α4-HDL, pre-α3-HDL, and α3-HDL) were associated with a higher risk plaque phenotype both by CTA and IVUS/VH, as evidenced by more NCP, a higher plaque volume, and more necrotic core, whereas the larger, more "mature" forms of HDL (pre-α2-HDL, α2-HDL, pre-α1-HDL, and α1-HDL) were associated with a less high-risk phenotype, as evidenced by less low-density NCP, a lower plaque volume, and less necrotic core. Finally, higher levels of pre-β2-HDL were associated with less stenosis and less necrotic core. Efficient reverse cholesterol transport is associated with the removal of more cholesterol from the vessel wall, leaving behind less lipid-rich and more calcified plaque. On the other hand, inefficient HDL maturation and/or HDL remodeling, marked by accumulation of the smaller, lipid-poor (α3- and α4-HDL) and low levels of the larger, lipid-rich (α1-HDL and α2-HDL) HDL subclasses, are associated with decreased reverse cholesterol transport and more lipid-rich atherosclerotic plaque.

Although the present study is the first to implement previously validated, quantitative plaque phenotyping with a combination of CTA and IVUS/VH and detailed lipoprotein analysis, such as 2D gel for HDL phenotyping, our findings are consistent with previously published data. Cheng et al[17] showed that increasing levels of LDL-C were associated with more noncalcified and less calcified plaque on CTA, similar to our findings. Furthermore, Shiga et al[18] showed that lower HDL levels were associated with more CTA-defined CAD in both statin-naive and statin-treated patients.

With regard to the role of HDL subclasses, our study is consistent with previously published data and expands on

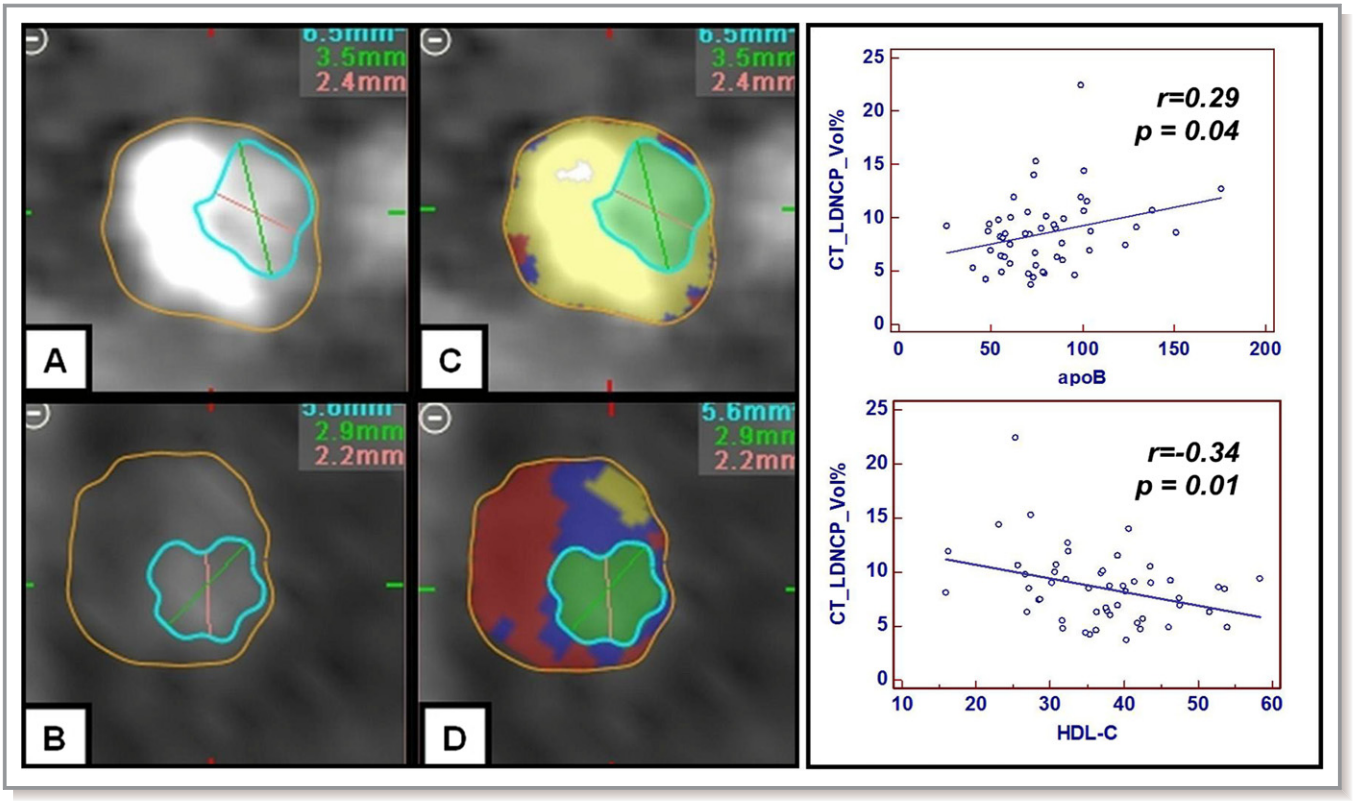

Figure 4. Correlation between CTA-derived low-density noncalcified plaque, apoB, and HDL-C. Increasing levels of apoB are associated with a shift from calcified (A and C) to more low-density noncalcified (B and D) plaque. Conversely, increasing levels of HDL-C are associated with less low-density noncalcified plaque (B and D). CTA indicates computed tomography angiography; HDL, high-density lipoprotein cholesterol; LD-NCP, low-density noncalcified plaque.

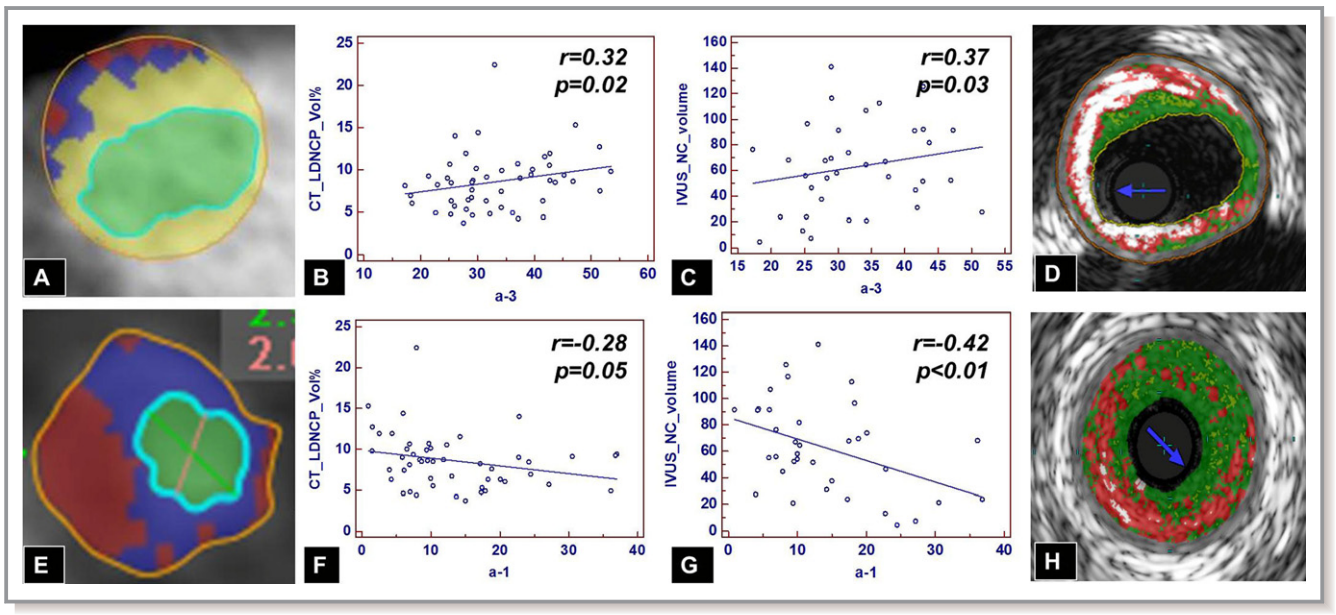

Figure 5. Correlation of small, dense, lipid-poor versus large, lipid-rich HDL particles and low-density noncalcified plaque on CTA and necrotic core on IVUS/VH. Increasing levels of small, dense, cholesterol-poor α3-HDL particles are associated with increasing amounts of low-density noncalcified plaque (B and E) and less calcified plaque (A) by CTA and with increasing amounts of necrotic core by IVUS/VH (C and D). Conversely, increasing levels of larger, cholesterol-rich α1-HDL particles are associated with less low-density noncalcified plaque by CTA (A and F) and less necrotic core by IVUS/VH (G and H). CTA indicates computed tomography angiography; HDL, high-density-lipoprotein; IVUS/VH, intravascular ultrasound virtual histology; LD-NCP, low-density noncalcified plaque; NC, necrotic core.

Table 5. IVUS/VH Characteristics of Coronary Atherosclerotic Plaques

IVUS/VH Parameter	Value, SD, IQR
Segment length, mm	63.0±18.9 (52.4 to 79)
Plaque volume, mm^3	433.6±178.1 (350.3 to 518.4)
Plaque burden, %	46.9±8.1 (43 to 51.8)
MLD, mm	1.76±0.42 (1.5 to 2.0)
MLA, mm^2	3.5±1.7 (2.5 to 4.3)
Dense calcium volume, mm^3	35.4±28.5 (15.4 to 48.3)
Fibrous tissue volume, mm^3	125.6±74.1 (56 to 144)
Fibrofatty tissue volume, mm^3	22.2±17.0 (10 to 26.8)
Necrotic core volume, mm^3	62.2±35.8 (31.2 to 91)
Dense calcium, %	13.8±7.5 (7.9 to 19.1)
Fibrous tissue, %	52.2±10.0 (46.8 to 58.7)
Fibrofatty tissue, %	9.2±5.5 (5.3 to 10.8)
Necrotic core, %	24.8±6.4 (21.3 to 28.9)

IQR indicates interquartile range; IVUS/VH, intravascular ultrasound virtual histology; MLA, minimal lumen area; MLD, minimal luminal diameter; SD, standard deviation.

those findings. Invasive coronary angiographic data from the HDL Atherosclerosis Treatment Study showed in 123 subjects that simvastatin-niacin treatment was associated with an increase in α1- and pre-α1-HDL and a decrease in pre-β1-HDL and α3-HDL, and these changes were associated with less angiographic atherosclerosis progression.[3] These findings are consistent with our findings of α1- and pre-α1-HDL associated with more benign and pre-β1-HDL and α3-HDL with less benign plaque phenotype by both CTA and IVUS/VH. Furthermore, Asztalos et al[4] demonstrated in the Framingham Offspring Study that high levels of α-1 and low levels of pre-β1- and α3-HDL were associated with less coronary heart disease, consistent with our findings. Finally, Asztalos et al also examined the association of HDL subpopulations with coronary events in the VA-HIT study in 398 subjects with and in 1097 subjects without recurrent events, showing that α1- and α2-HDL were associated with less and α3-HDL with more coronary heart disease events, consistent with our findings. These results taken together indicate that an inefficient remodeling of HDL particles may be associated with the removal of less cholesterol from atherosclerotic plaques, leaving behind more lipid-rich plaques, resulting in more progression of atherosclerosis and more cardiovascular events.

Our findings are also consistent with results from a recent publication by Khera et al[19], demonstrating that cholesterol efflux capacity, measured by a validated *ex vivo* essay, was an independent predictor of carotid artery wall thickness as measured by carotid intima-media thickness. Furthermore, efflux capacity was also an independent predictor of coronary disease status by invasive coronary angiography. Importantly, although efflux capacity was associated with apoAI and HDL-C levels, it remained an independent predictor even after adjusting for apoAI and HDL-C levels. Whereas high pre-β1 is a good acceptor of cholesterol from cells in *ex vivo* experiments, high pre-β1 level in vivo is a marker of inadequate HDL maturation and remodeling. Moreover, high

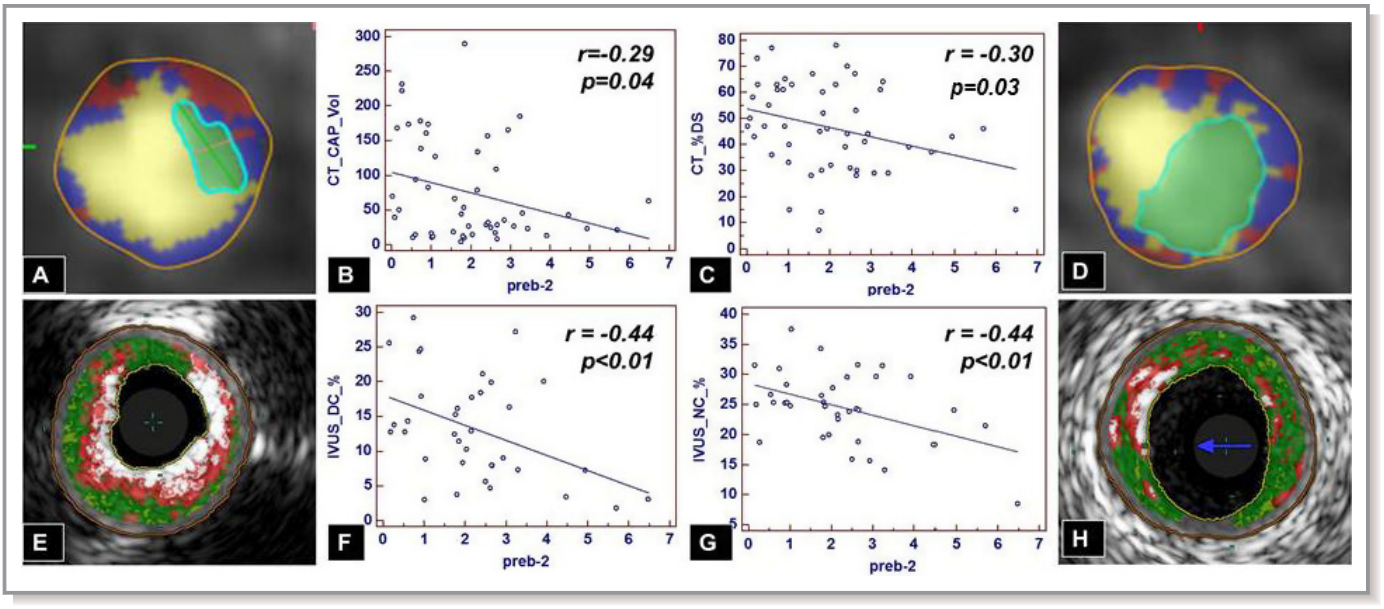

Figure 6. Pre-β2-HDL and plaque composition by CTA and IVUS/VH. On CTA, increasing levels of pre-β2-HDL particles are associated with less calcified plaque (A vs D and B) and smaller-diameter stenosis (A vs D and C). On IVUS/VH, increasing levels of pre-β2-HDL particles are associated with less dense calcium (E vs H and F) and less necrotic core (E vs H and G). CAP indicates calcified plaque; CTA, computed tomography angiography; DC, dense calcium; DS, diameter stenosis; HDL, high-density-lipoprotein; IVUS/VH, intravascular ultrasound virtual histology; LD-NCP, low-density noncalcified plaque; NC, necrotic core.

Table 6. Correlation Analysis Between Lipoproteins and IVUS-Derived Quantitative Coronary Atherosclerotic Plaque Parameters.

IVUS/VH Parameters	Biomarker	Univariate *r* Value	Univariate *P* Value	Multivariable β-Coefficient	Multivariable *P* Value	Adjusted *P* Value
Plaque volume	Lp(a)	0.42	0.01	2.7	0.03	0.03
	α4-HDL%	0.41	0.01	26.4	0.02	0.02
	α3-HDL%	0.37	0.03	8.8	0.07	0.07
	Pre-α2-HDL	−0.33	0.05	−33.4	0.02	0.02
	α1-HDL%	−0.41	0.01	−12.1	0.03	0.03
	α1-HDL	−0.44	<0.01	−7.6	0.03	0.03
	pre-α1-HDL%	−0.45	<0.01	−47.0	<0.01	<0.01
	Pre-α1-HDL	−0.48	<0.01	−33.4	<0.01	<0.01
Dense calcium volume	α4-HDL%	0.37	0.03	2.76	0.15	0.15
	Pre-α2-HDL	−0.39	0.02	−3.7	0.13	0.13
Fibrous tissue volume	Lp(a)	0.38	0.02	1.0	0.08	0.08
	LDL-C	0.34	0.04	1.36	<0.01	<0.01
	α4-HDL%	0.34	0.04	10.2	0.04	0.04
	α1-HDL%	−0.37	0.02	−4.8	0.05	0.05
	Pre-α1-HDL%	−0.37	0.03	−17	0.01	0.01
	α1-HDL	−0.37	0.03	−2.8	0.06	0.06
	Pre-α1-HDL	−0.39	0.02	−11.9	<0.01	<0.01
Fibrofatty tissue volume	Pre-α1-HDL%	−0.33	0.05	−4.0	0.01	0.01
	Pre-α1-HDL	−0.34	0.05	−2.74	0.01	0.01
Necrotic core volume	A4-HDL%	0.46	<0.01	5.1	0.02	0.02
	A3-HDL%	0.37	0.03	1.22	0.21	0.21
	Pre-α1-HDL	−0.34	0.04	−4.01	0.06	0.06
	α2-HDL	−0.35	0.03	−0.5	0.30	0.30
	Pre-α2-HDL	−0.38	0.02	−5.0	0.08	0.08
	α1-HDL%	−0.39	0.01	−2.0	0.06	0.06
	α1-HDL	−0.42	<0.01	−1.3	0.06	0.06
Dense calcium, %	Pre-α2-HDL	−0.33	0.05	−0.5	0.42	0.42
	Pre-β2-HDL%	−0.38	0.02	−3.2	0.01	0.01
	pre-β2-HDL	−0.44	<0.01	−2.2	0.01	0.01
Fibrous tissue, %	pre-β2-HDL	0.53	<0.01	3.47	<0.01	<0.01
	pre-β2-HDL%	0.47	<0.01	5.02	<0.01	<0.01
Necrotic core, %	A2-HDL%	−0.27	0.11	−0.21	0.32	0.32
	Pre-β2-HDL%	−0.37	0.03	−2.0	0.06	0.06
	Pre-β2-HDL	−0.44	<0.01	−1.6	0.03	0.03
MLA	Pre-α2-HDL	−0.33	0.05	−0.31	0.05	0.05
	Pre-α2-HDL%	−0.34	0.04	−0.46	0.04	0.04
%AS	Pre-β1-HDL	−0.32	0.03	−0.59	0.11	0.11
%DS	Pre-β1-HDL	−0.30	0.05	−0.39	0.15	0.15

Adjusted *P* values represent adjusting for age, sex, BMI, diabetes, and medication use. One multivariable model was fit for each biomarker separately. AS indicates area stenosis; BMI, body mass index; DS, diameter stenosis; HDL, high-density lipoprotein; IVUS/VH, intravascular ultrasound virtual histology; LDL-C, low-density lipoprotein cholesterol; Lp(a), lipoprotein a; MLA, minimal lumen area.

pre-β1 level in vivo is not the cause but the result of the impaired reverse cholesterol transport.

In summary, our findings provided complementary information to earlier data about the role of apoB- and apoA-containing lipoprotein subclasses and atherosclerotic plaque composition. Elevated levels of apoB-containing lipoproteins and a suboptimal HDL subpopulation profile were associated with a higher-risk plaque phenotype, with a higher proportion of noncalcified components and more coronary stenosis, as detected by CTA and IVUS/VH. Furthermore, it also provided additional external validation that the plaque components detected and quantified by contrast-enhanced CTA are biologically associated with lipoprotein metabolism, providing further support for the notion that CTA can adequately image lipid-rich atherosclerotic components. This was especially important with regard to the noncalcified plaque, particularly low-density NCP, detected by CTA, being associated with lipoprotein particles.

The role of HDL subclasses in the progression of atherosclerotic plaques needs to be evaluated in prospective clinical studies. Furthermore, careful evaluation of the changes in HDL subclasses during treatment with HDL-modifying therapies, such as niacin, cholesterol ester transfer protein inhibitors, and BAT inhibitors, should be included in clinical trials, and consideration should be given to including imaging surrogates in clinical outcomes trials of modifying the atherogenic milieu.

Limitations

Although our study was a prospective study, it has several limitations. It was a single-center study, and the number of patients was relatively small. Furthermore, for the purposes of this analysis, we only assessed patients in a cross-sectional fashion at 1 point in time. We only analyzed 1 prespecified lesion in each patient and not the entire coronary tree. Finally, the majority of patients were on lipid-lowering therapy at the time of imaging, mostly on medications affecting the apoB-containing lipoproteins. This may be partially responsible for the relative paucity of associations between apoB-containing particles and plaque characteristics, compared with the apoAI-containing particles.

Conclusions

In conclusion, our study showed a significant association between plaque characteristics and coronary stenosis by both CTA and IVUS/VH and with circulating lipoprotein particles. Higher levels of apoB-containing particles were associated with a higher proportion of noncalcified plaque and a lower proportion of calcified components. Impaired HDL remodeling, as evidenced by the accumulation of smaller, less mature HDL particles, was associated with a worse atherosclerotic phenotype by both CTA and IVUS/VH, whereas efficient remodeling of HDL particles was associated with a less high-risk phenotype and, ultimately, with less luminal stenosis with higher levels of pre-β2-HDL. Determination of more detailed lipoprotein parameters such as apoB, sd-LDL-C, and HDL particles by 2D gel electrophoresis may provide incremental clinical value beyond the measurements of the standard fasting lipid profile.

Sources of Funding

This study was supported by Abbott Vascular, Volcano Inc, Siemens Medical Systems, and Vital Images.

Disclosures

Szilard Voros: grant support from Abbott Vascular, Volcano, Inc, Siemens Medical Systems, Vital Images, Merck, Inc; consultant/advisory board for Vital Images, Merck, Inc, Health Diagnostics Laboratories, Inc; founder, owner, and CEO of Integrated Cardiovascular Research Group, LLC, and Global Genomics Group, LLC. Sarah Rinehart: grant support from Abbott Vascular, Volcano, Inc, Siemens Medical Systems, and Vital Images. Dimitri Karmpaliotis: grant funding from Medtronic; on speaker's bureau for Abbott Vascular. Michael Elashoff: employee of CardioDx, Inc, Palo Alto, CA. Ernst Schaefer, Bela Asztalos: stock options in Boston Heart Laboratory.

References

1. World Health Report 2002. 2002. Available at http://www.who.int/whr/2002/en. Accessed August 06, 2012.
2. Tabas I, Williams KJ, Boren J. Subendothelial lipoprotein retention as the initiating process in atherosclerosis: update and therapeutic implications. *Circulation*. 2007;116:1832–1844.
3. Asztalos BF, Batista M, Horvath KV, Cox CE, Dallal GE, Morse JS, Brown GB, Schaefer EJ. Change in alpha1 HDL concentration predicts progression in coronary artery stenosis. *Arterioscler Thromb Vasc Biol*. 2003;23:847–852.
4. Asztalos BF, Cupples LA, Demissie S, Horvath KV, Cox CE, Batista MC, Schaefer EJ. High-density lipoprotein subpopulation profile and coronary heart disease prevalence in male participants of the Framingham Offspring Study. *Arterioscler Thromb Vasc Biol*. 2004;24:2181–2187.
5. Asztalos BF, Collins D, Cupples LA, Demissie S, Horvath KV, Bloomfield HE, Robins SJ, Schaefer EJ. Value of high-density lipoprotein (HDL) subpopulations in predicting recurrent cardiovascular events in the Veterans Affairs HDL Intervention Trial. *Arterioscler Thromb Vasc Biol*. 2005;25:2185–2191.
6. Nair A, Kuban BD, Tuzcu EM, Shoenhagen P, Nissen SE, Vince DG. Coronary plaque classification with intravascular ultrasound radiofrequency data analysis. *Circulation*. 2002;106:2200–2206.
7. Akram K, Rinehart S, Voros S. Coronary arterial atherosclerotic plaque imaging by contrast enhanced computed tomography: fantasy or reality? *J Nucl Cardiol*. 2008;15:818–829.
8. Rinehart S, Vazquez G, Qian Z, Murrieta L, Christian K, Voros S. Quantitative measurements of coronary arterial stenosis, plaque geometry and composition are highly reproducible with a standardized coronary arterial computed tomographic approach in high-quality CT datasets. *J Comput Assist Tomogr*. 2010;5:35–43.
9. Rinehart S, Vazquez G, Qian Z, Voros S. Coronary plaque imaging with multislice computed tomographic angiography and intravascular ultrasound: a close look inside and out. *J Invasive Cardiol*. 2009;21:367–372.
10. Voros S, Rinehart S, Qian Z, Joshi P, Vazquez G, Fischer C, Belur P, Hulten E, Villines TC. Coronary atherosclerosis imaging by coronary CT angiography:

current status, correlation with intravascular interrogation and meta-analysis. *JACC Cardiovasc Imaging*. 2011;4:537–548.

11. Voros S, Rinehart S, Qian Z, Vazquez G, Anderson H, Murrieta L, Wilmer C, Carlson H, Taylor K, Ballard W, Karmpaliotis D, Kalynych A, Brown C III. Prospective validation of standardized, 3-dimensional, quantitative coronary computed tomographic plaque measurements using radiofrequency backscatter intravascular ultrasound as reference standard in intermediate coronary arterial lesions: results from the ATLANTA (assessment of tissue characteristics, lesion morphology, and hemodynamics by angiography with fractional flow reserve, intravascular ultrasound and virtual histology, and noninvasive computed tomography in atherosclerotic plaques) I study. *JACC Cardiovasc Interv*. 2011;4:198–208.
12. Stone GW, Maehara A, Lansky AJ, De Bruyne B, Cristea E, Mintz GS, Mehran R, McPherson J, Farhat N, Marso SP, Parise H, Templin B, White R, Zhang Z, Serruys PW. A prospective natural-history study of coronary atherosclerosis. *N Engl J Med*. 2011;364:226–235.
13. Ferencik M, Chan RC, Achenbach S, Lisauskas JB, Houser SL, Hoffmann U, Abbara S, Cury RC, Bouma BE, Tearney GJ, Brady TJ. Arterial wall imaging: evaluation with 16-section multidetector CT in blood vessel phantoms and ex vivo coronary arteries. *Radiology*. 2006;240:708–716.
14. Kashiwagi M, Tanaka A, Kitabata H, Tsujioka H, Kataiwa H, Komukai K, Tanimoto T, Takemoto K, Takarada S, Kubo T, Hirata K, Nakamura N, Mizukoshi M, Imanishi T, Akasaka T. Feasibility of noninvasive assessment of thin-cap fibroatheroma by multidetector computed tomography. *JACC Cardiovasc Imaging*. 2009;2:1412–1419.
15. Leber AW, Becker A, Knez A, von Ziegler F, Sirol M, Nikolaou K, Ohnesorge B, Fayad ZA, Becker CR, Reiser M, Steinbeck G, Boekstegers P. Accuracy of 64-slice computed tomography to classify and quantify plaque volumes in the proximal coronary system: a comparative study using intravascular ultrasound. *J Am Coll Cardiol*. 2006;47:672–677.
16. Asztalos BF, Roheim PS. Presence and formation of 'free apolipoprotein A-I-like' particles in human plasma. *Arterioscler Thromb Vasc Biol*. 1995;15:1419–1423.
17. Cheng VY, Wolak A, Gutstein A, Gransar H, Wong ND, Dey D, Thomson LE, Hayes SW, Friedman JD, Slomka PJ, Berman DS. Low-density lipoprotein and noncalcified coronary plaque composition in patients with newly diagnosed coronary artery disease on computed tomographic angiography. *Am J Cardiol*. 2010;105:761–766.
18. Shiga Y, Miura S, Mitsutake R, Kawamura A, Uehara Y, Saku K. Significance of serum high-density lipoprotein cholesterol levels for diagnosis of coronary stenosis as determined by MDCT in patients with suspected coronary artery disease. *J Atheroscler Thromb*. 2010;17:870–878.
19. Khera AV, Cuchel M, Llera-Moya M, Rodrigues A, Burke MF, Jafri K, French BC, Phillips JA, Mucksavage ML, Wilensky RL, Mohler ER, Rothblat GH, Rader DJ. Cholesterol efflux capacity, high-density lipoprotein function, and atherosclerosis. *N Engl J Med*. 2011;364:127–135.

Apoprotein B, Small-Dense LDL and Impaired HDL Remodeling Is Associated With Larger Plaque Burden and More Noncalcified Plaque as Assessed by Coronary CT Angiography and Intravascular Ultrasound With Radiofrequency Backscatter: Results From the ATLANTA I Study

Szilard Voros, Parag Joshi, Zhen Qian, Sarah Rinehart, Jesus G. Vazquez-Figueroa, Hunt Anderson, Michael Elashoff, Laura Murrieta, Dimitri Karmpaliotis, Anna Kalynych, Charles Brown, Ernst Schaefer and Bela Asztalos

J Am Heart Assoc. 2013;2:e000344; originally published November 19, 2013;
doi: 10.1161/JAHA.113.000344
The *Journal of the American Heart Association* is published by the American Heart Association, 7272 Greenville Avenue, Dallas, TX 75231
Online ISSN: 2047-9980